https://doi.org/10.25923/jkv3-gw89

Methods Report:
Assessing Community Risk in Relation to Coastal and Inland Natural Hazards in Maine's Washington County and Greater East Grand Region

October 2025

National Centers for Coastal Ocean Science
NOAA National Ocean Service
U.S. Department of Commerce

Suggested Citation

Fleming, C.S., Gunsher, R., Regan, S., Auerswald, K., and Freitag, A. (2025). Methods Report: Assessing Community Risk in Relation to Coastal and Inland Natural Hazards in Maine's Washington County and Greater East Grand Region. NOAA, National Ocean Service, National Centers for Coastal Ocean Science. https://doi.org/10.25923/jkv3-gw89

Authorship Credit

Supervision: C.F.; Project Administration: C.F.; Writing-Original Draft: C.F., R.G., S.R., K.A., A.F.; Validation: C.F., R.G.; Data Curation: R.G.; Formal Analysis: R.G., S.R., K.A., A.F.; Software: R.G., S.R., A.F.; Visualization: K.A., R.G.; Methodology: C.F., R.G., S.R., K.A., A.F.; Writing-Review & Editing: C.F., R.G., S.R., K.A., A.F.; Funding Acquisition: C.F.

Corresponding Author

Chloe Fleming, CSS Inc., under contract to NOAA NOS National Centers for Coastal Ocean Science
chloe.fleming@noaa.gov

Acknowledgments

We would like to thank our project partners from the Sunrise County Economic Council (SCEC), Maine Coast Heritage Trust, Maine Sea Grant at the University of Maine, Greater East Grand Economic Council, NOAA Office for Coastal Management, Washington County Emergency Management Agency, Downeast Salmon Federation, Maine Land Use Planning Commission, and Sipayik Resilience Committee for their support and regional expertise. We especially thank Tora Johnson (SCEC) for her technical guidance and local knowledge. We thank Heron Weston (formerly SCEC) for providing a guided tour of the study area and geospatial landscape; Tora Johnson, Jen Peters, and Tanya Rucoscy (SCEC) for workshop logistical support; and Jessica Brunacini (Wells National Estuarine Research Reserve—formerly Maine Sea Grant) for liaising initiation of this project and connecting us with key partners. We also thank Tora Johnson (SCEC), Jamie Carter (NOAA Office for Coastal Management), Chandra Goetsch (CSS/NOAA NCCOS), and Matt Poti (NOAA NCCOS) for their technical review, Sarah Gonyo and Theresa Goedeke (NOAA NCCOS) for their project support and policy review, and Ginger Shoup (CSS/NOAA NCCOS) for copy editing and formatting support.

Cover image credits: Reilee Gunsher (CSS/NOAA NCCOS)

Disclaimer

Any use of trade, firm, or product names is for descriptive purposes only and does not imply endorsement by the U.S. Government.

Methods Report:
Assessing Community Risk in Relation to Coastal and Inland Natural Hazards in Maine's Washington County and Greater East Grand Region

Authors

Chloe Fleming,[1] Reilee Gunsher,[1] Seann Regan,[1] Katie Auerswald,[1] and Amy Freitag[2]

[1] *CSS, Inc., under contract to NOAA, National Ocean Service, National Centers for Coastal Ocean Science*

[2] *NOAA, National Ocean Service, National Centers for Coastal Ocean Science*

October 2025

National Centers for Coastal Ocean Science
NOAA National Ocean Service
U.S. Department of Commerce

Table of Contents

1. Data Overview and Accessibility

This methods report accompanies this assessment's data archival package and summarizes all project methods and datasets. Table 1 provides a quick reference for this assessment's archived data, available through Harvard Dataverse (https://doi.org/10.7910/DVN/SICI8E) and https://www.data.gov. Any non-derived datasets referenced throughout this report are publicly available and are not included in the table below.

Table 1. *Derived indices, indicators, and datasets by thematic category.*

Thematic Category	Indices, Indicators, and Datasets	Data Type
Study area	NCCOS Maine risk assessment study area	Polygon
	Study area territories	Polygon
Population	Population density index	30-m raster
Structural	Structural index	Point
	Structural density index	30-m raster
Hazard	Storm surge hazard index	30-m raster
	Stormwater flood hazard index	30-m raster
	Flow accumulation indicator	30-m raster
	Rainfall intensity indicator	30-m raster
	Geology (hydrologic soil group) indicator	30-m raster
	Land use/land cover indicator – stormwater	30-m raster
	Slope indicator	30-m raster
	Elevation indicator – stormwater	30-m raster
	Drainage network indicator	30-m raster
	Winter Ice storm hazard index	30-m raster
	Winter precipitation indicator	30-m raster
	Elevation indicator – ice storm	30-m raster
	Land use/land cover indicator – ice storm	30-m raster
	Wildfire hazard index	30-m raster
Structural hazard risk	Compounded hazard structural risk index	Point
	Storm surge hazard structural risk index	Point
	Stormwater flood hazard structural risk index	Point
	Wildfire hazard structural risk index	Point
	Winter ice storm hazard structural risk index	Point
	Compounded hazard structural risk index – excluding storm surge	Point
Road-stream crossings	Soil erodibility index	30-m raster
	Hydrologic soil group indicator	30-m raster
	Wind erodibility group indicator	30-m raster
	Drainage class indicator	30-m raster
	Stormwater/erodibility index	30-m raster
	Modeled roads	Polyline

Thematic Category	Indices, Indicators, and Datasets	Data Type
	Comprehensive road-stream crossings	Point
	Road-stream crossing risk index	Point
	Road-stream crossing density	30-m raster
	Road-stream crossing risk index – stormwater flooding only	Point
	Road-stream crossing risk index – soil erodibility only	Point
Community isolation	Routable road network	File geodatabase network dataset
	Routable roads	Polyline
	Routable road junctions	Point
	Road segment isolation index	Polyline
	Compounded hazard road isolation risk index	Polyline
	Stormwater flooding road isolation risk index	Polyline
	Winter ice storm road isolation risk index	Polyline
	Wildfire road isolation risk index	Polyline
	Road-stream crossings road isolation risk index	Polyline
	Overall service area isolation risk index	Polyline
	Health-based service area isolation risk index	Polyline
	Order/safety-based service area isolation risk index	Polyline
	Services-based service area isolation risk index	Polyline
Co-occurrence	Population density index by group class	30-m raster
	Storm surge hazard index by group class	30-m raster
	Stormwater flood hazard index by group class	30-m raster
	Winter ice storm hazard index by group class	30-m raster
	Wildfire hazard index by group class	30-m raster
	Soil erodibility index by group class	30-m raster

Road damage in Washington County, Maine. Credits: (left) Reilee Gunsher (CSS/NOAA NCCOS); (right) Chloe Fleming (CSS/NOAA NCCOS).

2. Project Background

United States coastal counties are exposed to a variety of environmental hazards, such as coastal and inland flooding, erosion, wildfire, and coastal storms. The National Centers for Coastal Ocean Science (NCCOS) conducts place-based integrated community risk assessments to help coastal counties understand their unique risks (Fleming et al., 2017; Fleming et al., 2024; Fleming et al., 2020). In 2024, NCCOS scientists began their seventh community risk assessment for Maine's Washington County and Greater East Grand Region. Figure 1 shows the **Study Area Territories** (polygons) within Maine's Aroostook, Penobscot, and Washington Counties (Pettit and State of Maine, 2021b), described in Table 2. The team selected these territories and clipped the 3-nautical-mile buffer from the coastal areas using the Maine State boundary shapefile (Pettit and State of Maine, 2021a). All 90 territory boundaries were then dissolved to create the **NCCOS Maine Risk Assessment Study Area** boundary (polygon), projected in NAD 1983 UTM Zone 19N (Figure 1)**.**

Table 2. *Study area territories.*

Territories	County		
	Washington	**Aroostook**	**Penobscot**
Towns	41	4	0
Townships	35	3	1
Plantations	2	2	0
Native American Reservations	2	0	0
Total Territories	**80**	**9**	**1**

To inform the project scoping process following project kickoff in June 2024, the research team held an in-person workshop in August and virtual follow-up consultations in September with a variety of project partners (Table 3). Participants were invited to provide input based on expertise, organization, interest, and availability within Washington County and the wider planning region. After additional data availability and feasibility checks, the project team began analysis to assess the following: population density, critical infrastructure, coastal storm surge from a Category 2 hurricane, precipitation-based stormwater flood potential, winter ice storm hazard, wildfire hazard, road-stream crossing erosion risk, community isolation risk, and co-occurrence mapping.

Turkeys in Washington County, Maine. Credit: Reilee Gunsher (CSS/NOAA NCCOS).

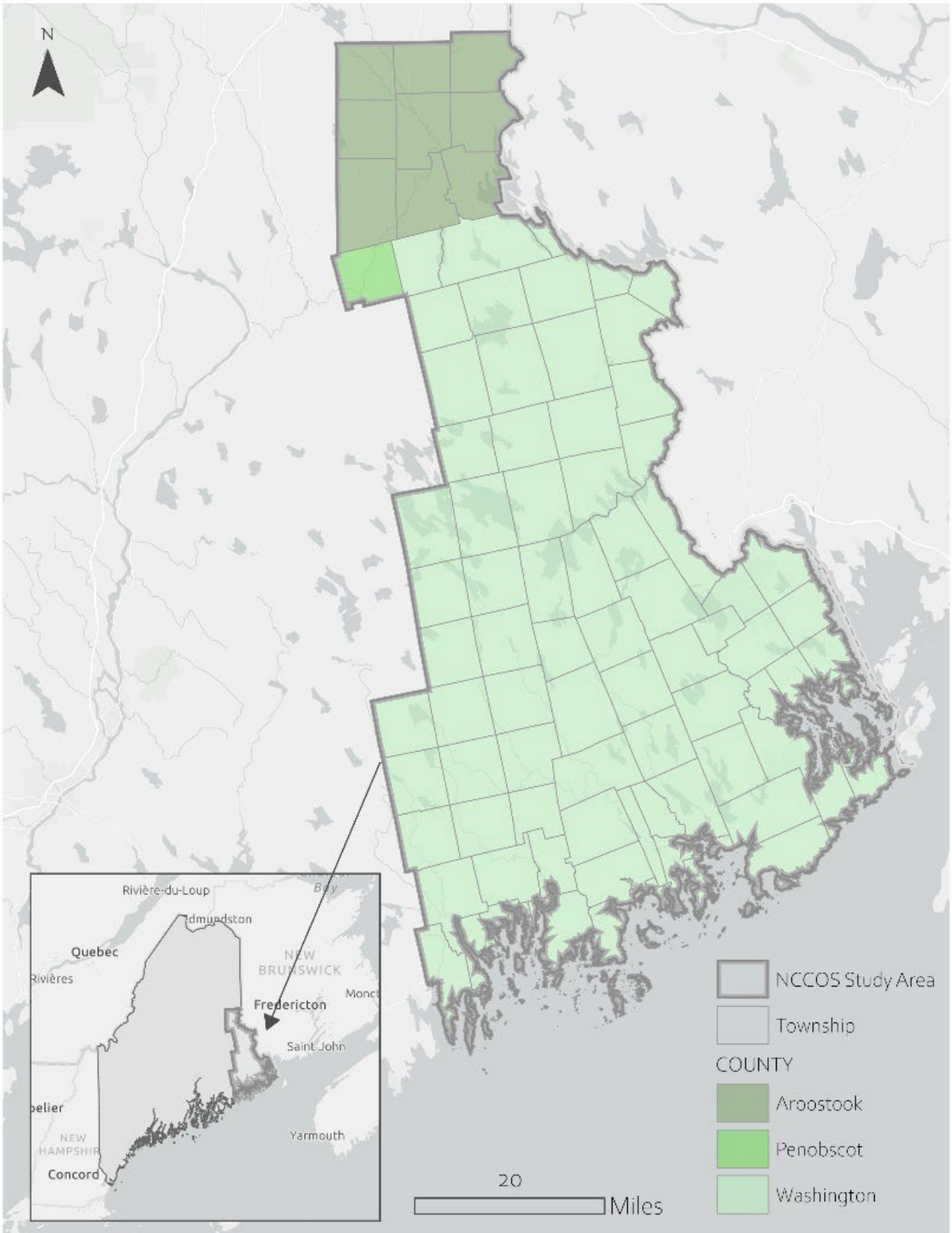

Figure 1. *Study area: Washington County and Greater East Grand Region. Study area geographic extent – northern boundary: 46.8230274, southern Boundary: 43.3423063, western boundary: −70.4638597, eastern boundary: −64.8663419.*

Table 3. *Project partners that contributed to the scoping of the risk assessment.*

	Participating Organizations	Number of Participants
In-person workshop	Sunrise County Economic Council	3
	Maine Coast Heritage Trust	1
	Maine Sea Grant at the University of Maine	1
	Greater East Grand Economic Council	1
	NOAA Office for Coastal Management	1
	Maine Aquaculture Innovation Center*	1
	Wells National Estuarine Research Reserve*	1
Follow-up consultation	Washington County Emergency Management Agency	1
	Downeast Salmon Federation	2
	Downeast Region Land Use Planning Commission	2
	Sipayik Resilience Committee	1
	Sunrise County Economic Council	1
	Total	**16**

**Observation only*

Workshop mapping exercise. Credit: Reilee Gunsher (CSS/NOAA NCCOS).

3. Methods

Following portfolio standards (NOAA National Centers for Coastal Ocean Science, 2025), this report uses the following definitions of hazard and risk:

> **Hazard**: An event or condition that may cause injury, illness, or death to people or damage to assets (U.S. Climate Resilience Toolkit, n.d.).
>
> **Risk**: The potential for negative consequences from adverse weather-related events or other natural hazards where something of value is at stake (adapted from U.S. Climate Resilience Toolkit (n.d.)).

Each assessment component was quantified using indicators and indices derived from the most recent, publicly available data. All spatial data processing was conducted in ArcGIS Pro version 3.4.0 and clipped using either a study-area vector boundary or a 30×30-m raster mask.

Data inputs were available at 30-m resolution or finer, with the exception of population density (100 m) and precipitation (800 m). To evaluate tradeoffs in spatial precision and applicability, two test indicators (precipitation and land use/land cover) were analyzed at both original and rescaled resolutions. Resampling precipitation resolution from 800 m to 30 m reduced blocky, stair-step artifacts while preserving spatial trends and overall pixel values. Conversely, aggregating 30-m land use/land cover data to 1-km generated artificial mean values that obscured genuine spatial heterogeneity. Based on these results and partner requirements, all inputs were retained at a 30-m resolution to ensure spatial congruence and facilitate coherent relative analyses. It is noted that resampling does not enhance the intrinsic spatial detail of the original precipitation and population density data, and it is explicitly stated that the stormwater flooding and winter ice storm hazard indices integrate precipitation data derived at a coarser resolution, alongside 30-m inputs.

Raster outputs were snapped or resampled to a 30×30-m-resolution raster using bilinear interpolation, unless otherwise specified. Vector outputs were presented as points or lines. Indicators were normalized through minimum-maximum (min-max) normalization from 0–1, following ArcGIS best practices (ESRI, 2023). Where appropriate, indicators were combined into composite indices using weighted approaches described in the subsequent sections. Resulting values were then categorized into statistical quantile breaks to communicate relative scores across each index (i.e., low, medium, high). Please view the full archival package for the corresponding data dictionary for this report.

3.1 Population Density

The research team utilized population density data between 2000–2020 from WorldPop (2022). This data source produces gridded population data using a Random Forest-based dasymetric redistribution approach that combines census-based population counts with ancillary geospatial data, such as land cover and infrastructure, to model where people are likely to be located within each grid cell (Stevens et al., 2015; WorldPop, 2022). The Random Forest algorithm is used to identify relationships between population density and these spatial covariates, enabling redistribution of population counts at a finer spatial resolution and highlighting general

trends in population distribution rather than exact locations where individuals live or work. The resulting population density surfaces should be interpreted as modeled approximations for spatial analysis and relative comparison (WorldPop, 2022). WorldPop population density data were available at a 100×100-m spatial resolution. The data were clipped and resampled using nearest neighbor resampling because this approach preserves discrete values, avoids introducing unrealistic fractional counts, and maintains the integrity of population boundaries. The data were then rescaled from 0–1 through min-max normalization, resulting in a **population density index** in 30×30-m resolution. Because this indicator uses coarser 100-m resolution data, it should only be used to assess broad geographic trends.

3.2 Critical Infrastructure

The research team developed a structural index that examines the distribution of critical infrastructure throughout the study area. Project workshops (see Section 2) determined the most important critical infrastructure to include, building upon infrastructure already included in Washington County's planning maps' public services layer (Sunrise County Economic Council, n.d.). Selected structural indicators are summarized in Table 4.

Table 4. *Structural indicators.*

Indicator	Source
Ambulance services	(Johnson and Sunrise County Economic Council, 2025)
County emergency management agencies	(Bistrais and State of Maine, 2022)
Fire stations	(Bistrais and State of Maine, 2022)
Emergency medical service (EMS) stations	(Bistrais and State of Maine, 2022)
Hospitals	(Bistrais and State of Maine, 2022)
Law enforcement facilities	(Pettit and State of Maine, 2025)
Assisted living and nursing homes	(Bistrais and State of Maine, 2021d)
Government offices	(Bistrais and State of Maine, 2022)
Childcare providers	(Johnson and Sunrise County Economic Council, 2025)
Early childhood education facilities	(University of Maine Machias, 2021)
Schools	(Bistrais and State of Maine, 2022)
Colleges and universities	(Bistrais and State of Maine, 2022)
Libraries	(Bistrais and State of Maine, 2021b)
Post offices	(ESRI Business Analyst Data Axle, 2024d)
Correctional facilities	(Bistrais and State of Maine, 2021a)
Grocery stores	(ESRI Business Analyst Data Axle, 2024b)
Hardware stores	(ESRI Business Analyst Data Axle, 2024a)
Gas stations	(ESRI Business Analyst Data Axle, 2024c)
Laundries	(ESRI Business Analyst Data Axle, 2024e)

Indicator	Source
Hazardous materials sites (from the Environmental Protection Agency's Facility Registry Service)[1]	(U.S. Environmental Protection Agency, 2024)
Dams	(ESRI ArcGIS REST Services Directory, 2025)
Power lines	(University of Maine Machias, 2020)
Cemeteries	(Bistrais and State of Maine, 2021c)
Roads	(Bistrais and State of Maine, 2022)
Recovery treatment health providers	(ESRI Business Analyst Data Axle, 2024g)
Psychiatry and psychopharmacology providers	(ESRI Business Analyst Data Axle, 2024f)
Farmers markets	(Maine Federation of Farmers Markets, 2025)
Cultural and historical sites (through the National Registry of Historic Places)	(ESRI ArcGIS REST Services Directory, 2024)
Public health offices	(Bistrais and State of Maine, 2022)

To approximate nonpoint infrastructure coverage, polyline layers were clipped and converted to point layers by generating points every 30 m along each line (*Generate Points Along Lines* tool). (For more spatially explicit analyses regarding road infrastructure, see Sections 3.8 and 3.9.) The resulting new points layers were merged with all other clipped points layers to produce a **structural index** (points). The *Kernel Density* tool was then used to develop a heat map of critical infrastructure density, resulting in a **structural density index** map in 30×30-m resolution.

3.3 Storm Surge Hazard

Following destructive January 2024 storms that brought record flooding and high winds to coastal Maine (National Weather Service, 2024; Santom, 2025), partners prioritized Category 2 hurricane storm surge modeling to plan for extreme conditions. To estimate coastal flooding hazard, the research team incorporated Category 2 storm surge data from the State of Maine Geological Survey (2019) geoportal.[2] Data were available as categorical vector shapefiles and were clipped and rasterized at a 30×30-m resolution (*Feature to Raster* tool). Rasterized data were visualized into equal inundation depth bins of 3 ft to preserve the original vector values, resulting in a **storm surge hazard index** in 30×30-m resolution. Raster cells beyond the extent of the original vector shapefiles were assigned null values.

[1] See the EPA Facility Registry Service for a list a included sites. U.S. Environmental Protection Agency. (2024). *FRS_Interests (FeatureServer)* (https://services.arcgis.com/cJ9YHowT8TU7DUyn/arcgis/rest/services/FRS_INTERESTS/FeatureServer).

[2] These data originated from the Sea Lake and Overland Surges from Hurricanes (SLOSH) Scenarios developed by the NOAA National Hurricane Center. (n.d.). *National Storm Surge Risk Maps – Version 3*. Retrieved 19 September 2025 from https://www.nhc.noaa.gov/nationalsurge/#:~:text=The%20process%20to%20create%20storm,a%20seamless%20raster%20of%20inundation

3.4 Stormwater Flood Hazard

To examine precipitation-based stormwater flooding in both coastal and inland areas, the research team applied the FIGUSED methodology by Kazakis et al. (2015) to develop a stormwater flood hazard index. The FIGUSED methodology integrates seven critical indicators to assess flood hazard potential related to precipitation:

- Flow accumulation (F)—a measure used to delineate a drainage area (Jenson and Domingue, 1988);
- Rainfall intensity (I)—a measure of the amount of precipitation within a given amount of time and at peak values that can approximate runoff rates (Conkle et al., 2006);
- Geology through hydrologic soil groups (G)—categorizations of soils that influence their permeability and runoff potential (U.S. Department of Agriculture Natural Resources Conservation Service, 2019b);
- Land use (U)—land use/land cover types that determine their likelihood of being flood prone or commonly associated with wetlands (Kazakis et al., 2015);
- Slope (S)—a measure that influences water drainage potential (Kazakis et al., 2015); flatter slopes and low elevations are more likely to experience flooding due to slower drainage and higher water tables;
- Elevation (E)—a measure that relates to water table height (Kazakis et al., 2015); and
- Proximity to drainage networks (D)—a measure thought to influence likelihood of flooding through adjacency (Kazakis et al., 2015).

Flow accumulation (F) was developed from a 30×30-m digital elevation model (DEM) derived from U.S. Geological Survey 3D Elevation Program tiles (U.S. Geological Survey, 2023b, 2023c, 2023d, 2024a, 2024b). The research team clipped the data to the study area and filled sinks (imperfections) in the data (*Fill Function*). These sinks are errors in elevation data where water wrongly appears to collect, and filling sinks to correct these imperfections allows for realistic water flow analysis (Sharma and Tiwari, 2019). The team then calculated the flow direction and flow accumulation. Polylines were created from the raster, and the raster was rescaled from 0–1 using min-max normalization to produce a **flow accumulation indicator** in 30×30-m resolution.

Rainfall intensity (I) was developed from 800×800-m resolution 30-year precipitation normals data from the PRISM Climate Group at Oregon State University (2022a). Data were clipped, resampled to 30×30-m resolution using bilinear interpolation, and rescaled from 0–1 using min-max normalization to produce a **rainfall intensity indicator** in 30×30-m resolution. Because this indicator uses coarser 800-m resolution data, it should be used only as an input for the stormwater flood hazard index or to assess broad geographic trends.

Hydrologic soil group polygons (G) were downloaded from the U.S. Department of Agriculture Soil Survey Geographic Database (U.S. Department of Agriculture Natural Resources Conservation Service, 2019b) and clipped to the study area. Per USDA soil definitions (U.S. Department of Agriculture Natural Resources Conservation Service, 2019b), the research team assigned a value of 0 to polygon areas with soil hydrologic groups A and B, as these are considered well drained, and assigned a value of 1 to polygon areas with soil hydrologic groups C and D, as these soils have lower permeability and increased runoff potential. A value of 1 was also assigned to polygon areas with soil hydrologic groups A/D, B/D, and C/D, as dual groupings generally represent wet soils based on the presence and depth of the water table. Polygons were then rasterized to 30×30-m resolution (*Feature to Raster* tool) and rescaled from 0–1 using min-max normalization, producing a **geology (hydrologic soil group) indicator** in 30×30-m resolution.

Land use (U) was developed from 30×30-m resolution data from the U.S. Geological Survey Earth Resources Observation and Science Center (2024). The data were clipped to the study area and reclassified based on their flooding potential as suggested in Kazakis et al. (2015) (Table 5), producing a **land use/land cover indicator – stormwater** in 30×30-m resolution.

Table 5. *Land use/land cover type reclassification crosswalk for stormwater flooding potential.*

Land Use/ Land Cover Value	Reclassified Value for Stormwater Flooding Potential
11 (Open Water)	1
21 (Developed, Open space)	0.5
22 (Developed, Low Intensity)	0.5
23 (Developed, Medium Intensity)	0.5
24 (Developed, High Intensity)	1
31 (Barren Land, Rock/Sand/Clay)	0.8
41 (Deciduous)	0.2
42 (Evergreen Forest)	0.2
43 (Mixed Forest)	0.2
52 (Shrub/Scrub)	0.2
72 (Sedge/Herbaceous)	0.4
81 (Pasture/Hay)	0.6
82 (Cultivated Crops)	0.6
90 (Woody Wetlands)	1
95 (Emergent Herbaceous Wetlands)	1

Slope (S) and elevation (E) indicators were both developed from the same clipped 30×30-m DEM described above (U.S. Geological Survey, 2023b, 2023c, 2023d, 2024a, 2024b). Percent slope and elevation values were respectively rescaled from 0–1 using min-max normalization and inverted so that steeper slope and higher elevation decreased flooding potential. This resulted in a **slope indicator** and an **elevation indicator–stormwater,** both in 30×30-m resolution.

Lastly, distance from the drainage network (D) was calculated from the U.S. Geological Survey's National Map (2021) rivers and streams data (polylines) (*Line Density* tool). The research team rescaled the distance from rivers and streams from 0–1 using min-max normalization, with closer distances more proximal to potential water overflows. This produces a **drainage network indicator** in 30×30-m resolution.

These 7 indicators were equally weighted in an additive index from 0-7 to produce a final **stormwater flood hazard index** in 30×30-m resolution. Please note that this index incorporates coarser 800-m resolution precipitation data.

3.5 Winter Ice Storm Hazard

To approximate ice storm hazard, the research team developed an index methodology based on the scientific literature (Cortinas Jr. et al., 2004; Degelia et al., 2016; Isaacs et al., 2014; McCray et al., 2019). The developed index integrated three climatic and environmental indicators to identify areas where ice accumulation is more likely to occur and cause more damage during winter months:

- Precipitation intensity – increased precipitation raises the likelihood of more severe ice accumulation (McCray et al., 2019) when coupled with below-freezing temperatures;
- Elevation – higher elevation increases the likelihood of freezing conditions (DeGaetano et al., 2002); and
- Vegetation cover – forested areas increase the likelihood of ice accumulation impacts from downed trees and disrupted power lines, with the potential for greater damage (Irland, 2000);

Since temperatures between −8°C and 0°C increase the likelihood of ice formation (Cortinas Jr. et al., 2004), incorporation of air temperature during winter months was also considered. Monthly 30-year temperature normals for December, January, and February, however, were all at or below freezing (within the range mentioned above) (PRISM Climate Group at Oregon State University, 2022b, 2022d, 2022f), and colder subfreezing temperatures are not shown to be more likely to result in freezing rain than warmer subfreezing temperatures (Cortinas Jr. et al., 2004). As a result, temperature was excluded, and the final index captures a proxy for the relative likelihood of ice storm hazard *during freezing conditions*. Additionally, the research team was unable to access spatially explicit vertical temperature data that also contribute to the likelihood of freezing rain (National Weather Service, n.d.).

Average monthly precipitation data were sourced from the PRISM Climate Group at Oregon State University (2022c, 2022e, 2022g) for the months of December, January, and February in 800×800-m resolution. Data were limited to winter months to capture seasonality of ice storm frequency on the east coast (DeGaetano et al., 2002). Average monthly precipitation data in millimeters per hour were clipped, resampled to 30×30-m resolution using bilinear interpolation, and rescaled from 0–1 using min-max normalization to produce a **winter precipitation indicator** in 30×30-m resolution. Because this indicator uses coarser 800-m resolution data, it should be used only as an input for the winter ice storm hazard index or to assess broad geographic trends.

The research team used a clipped 30×30-m DEM from the U.S. Geological Survey (2023b, 2023c, 2023d, 2024a, 2024b) to measure elevation and land use/land cover data from the U.S. Geological Survey Earth Resources Observation and Science Center (2024) to assess land cover types. Elevation was rescaled from 0–1 using min-max normalization, with higher elevations ranked as more susceptible to icing (DeGaetano et al., 2002). This resulted in an **elevation indicator – ice storm** in 30×30-m resolution. Table 6 shows the reclassification of 30×30-m land use/land cover values to estimate ice storm hazard susceptibility based on the Winter Storm Severity Index (Weather Prediction Center, n.d.). The ice accumulation component of this index addresses impacts resulting from ice accretion on flat and elevated surfaces, which can include disruptions to surface transportation, pedestrian injuries, and damage to property and vegetation (Weather Prediction Center, 2025). Tree type and density were considered as well. Higher values were assigned to deciduous trees due to their increased surface area of lateral branches and broad crowns, which are more prone to breakage (Hauer et al., 2006). Evergreen forests typically have smaller crowns and are more resilient to ice accumulation, and were assigned slightly lower values as a result. Reclassified values were rescaled from 0–1 using min-max normalization, resulting **land use/land cover indicator – ice storm** in 30×30-m resolution.

Ultimately, these three indicators were equally weighted in an additive index to produce a final **winter ice storm hazard index** from 0–3 in 30×30-m resolution. This index does not directly assess the potential for ice storms beyond the months of December to February, and it incorporates coarser 800-m resolution data.

Table 6. *Land use/land cover types reclassification crosswalk for ice storm hazard potential.*

Land Use/Land Cover Value	Reclassified Value for Ice Accumulation Impact via Winter Storm Severity Index
11 (Open Water)	0
21 (Developed, Open space)	0
22 (Developed, Low Intensity)	0.5
23 (Developed, Medium Intensity)	0.6
24 (Developed, High Intensity)	0.7
31 (Barren Land, Rock/Sand/Clay)	0
41 (Deciduous)	1
42 (Evergreen Forest)	0.8
43 (Mixed Forest)	0.9
52 (Shrub/Scrub)	0
72 (Sedge/Herbaceous)	0
81 (Pasture/Hay)	0
82 (Cultivated Crops)	0
90 (Woody Wetlands)	0
95 (Emergent Herbaceous Wetlands)	0

3.6 Wildfire Hazard

The research team utilized a 30×30-m burn probability dataset developed by the USDA Forest Service Rocky Mountain Research Station and Pyrologix LLC (Scott et al., 2024). This dataset uses fire simulation modeling to model over 20,000 fire seasons across 136 distinct U.S. wildfire activity regions. Scott et al. (2024) calibrated the simulations using fire occurrence data from 2006–2020 to highlight the annual likelihood of a wildfire occurring at a specific location, and then assigned non-zero values to burnable pixels and a value of zero to non-burnable pixels. The NCCOS team clipped these data to the study area and rescaled them from 0–1 using min-max normalization, resulting in a **wildfire hazard index** in 30×30-m resolution.

3.7 Structural Risk by Hazard

Using the structural index (see Section 3.2) and the final storm surge, stormwater flood, wildfire, and ice storm hazard raster indices (see Sections 3.3–3.6), the team created structural risk indices for each hazard by extracting raster values from each hazard index at each point location within the structural index. Because the final storm surge values were categorical, reclassified values from 1–4 for each storm surge raster pixel category (with null values converted to 0) were applied to structural index points. The resulting risk values were rescaled from 0–1 using min-max normalization, where higher values equal higher structural risk due to the respective hazard. This resulted in four new indices: **storm surge hazard structural risk** (points), **stormwater flood hazard**

structural risk (points), **wildfire hazard structural risk** (points), and **winter ice storm hazard structural risk** (points). These indices were further combined into equally additive compounded risk indices of **compounded hazard structural risk** (points) from 0–4**,** and **compounded hazard structural risk** – **excluding storm surge** (points) from 0–3.

3.8 Road-Stream Crossing Risk

The research team developed a road-stream crossing risk index based on Panda et al.'s (2022) streambank erosion vulnerability assessment model. Panda et al.'s (2022) comprehensive geospatial-hydrology model uses a Delphi-based weighted-probability scale to integrate four critical indicators to assess streambank erosion vulnerability: precipitation, soil, elevation, and land use/land cover data. NCCOS's model followed a modified approach to accommodate existing assessment components and data limitations. Both models incorporate measures of precipitation, drainage, elevation, slope, land use/land cover, and soil properties. Differences between the two models are shown in Table 7. For example, because K-factor data (measurements of soil susceptibility to erosion by rainfall and surface runoff) used in the Panda et al. (2022) model were not available for the entirety of the team's study area, the team substituted other data to inform a soil erodibility index. This index and the team's stormwater flood hazard index were combined to inform risk scores for every road-stream crossing point. This approach intentionally double-weighted hydrologic soil groups as they are included within both indices, contributing about 33% to the soil erodibility index and about 14% to the stormwater flood hazard index. In each index, these soil groups serve different roles: In the soil erodibility index, they act as a proxy for water erodibility (due to a lack of K-factor data for the study area), while in the flood hazard index, they reflect infiltration depth and permeability.

Roques Bluff culvert. Credit: Reilee Gunsher (CSS/NOAA NCCOS).

Table 7. *Data inputs for Panda et al.'s (2022) streambank erosion model and the research team's road-stream crossings model.*

Model	Data Inputs	
Streambank Erosion Vulnerability Assessment Model (Panda et al., 2022)	Soil properties	K-factor
		Hydrologic soil group
		Soil texture
		Slope length
		Drainage
	Land use/land cover	
	Annual average precipitation	
	Digital elevation model	
Road-Stream Crossing Risk Potential Model	Soil erodibility index	Hydrologic soil group
		Wind erodibility group
		Drainage class
	Stormwater flood hazard index	Flow accumulation
		Rainfall intensity
		Hydrologic soil group
		Land use/land cover
		Slope
		Elevation
		Distance from drainage network

3.8.1 Soil Erodibility Index

To examine soil erodibility, the research team incorporated hydrologic soil group (2019b), wind erodibility group (2019c), and drainage class (2019a) soil data from the U.S. Department of Agriculture National Resources Conservation Service Soil Survey Geographic Database. Hydrologic soil group and drainage class communicate different aspects of soil susceptibility to water-based erosion factors, and wind erodibility group reflects a soil's susceptibility to erosion caused by wind, based on texture and other physical characteristics (National Resources Conservation Service Soil Survey Staff, 2023). Each dataset was converted from polygons to a raster (*Feature to Raster* tool), and each resulting raster was reclassified from 1–7 following the reclassification crosswalks shown in Table 8, Table 9, and Table 10 to preserve the categorical values of the source data. This resulted in a **hydrologic soil group indicator,** a **drainage class indicator,** and a **wind erodibility group indicator,** all in 30×30-m resolution. These indicators were then assigned equal weights and summed to produce a **soil erodibility index** in 30×30-m resolution from 1–7.

Blueberry barren. Credit: Reilee Gunsher (CSS/NOAA NCCOS).

Table 8. *Hydrologic soil group rating reclassification crosswalk for soil erodibility potential.*

Hydrological Soil Group Rating	Soil Type	Reclassified Value
A	High infiltration rate and high permeability (e.g., deep, well-drained sands)	1
A/D	Type A when drained; type D when undrained	2
B	Moderate infiltration rate and moderate permeability (e.g., moderately deep, moderately well-drained soils)	3
B/D	Type B when drained; type D when undrained	4
C	Slow infiltration rate and low permeability (e.g., sandy clay loams)	5
C/D	Type C when drained; type D when undrained	6
D	Very slow infiltration rate and very low permeability (e.g., clay soils)	7

Table 9. *Drainage class reclassification crosswalk for soil erodibility potential.*

Drainage Class Description	Reclassified Value
Excessively drained	1
Somewhat excessively drained	2
Well drained	3
Moderately well drained	4
Somewhat poorly drained	5
Poorly drained	6
Very poorly drained	7

Table 10. *Wind erodibility group reclassification crosswalk for soil erodibility potential.*

Wind Erodibility Group	Reclassified Value
1	1
2	2
3	3
5	4
6	5
7	6
8	7

3.8.2 Comprehensive Road-Stream Crossings and Risk

The research team developed a comprehensive dataset of the study area's road-stream crossings. First, the team added a 3-nautical-mile buffer to the study area to avoid excluding road-stream crossings that extended across littoral and riverine boundaries. Next, the State of Maine's emergency 911 roads feature class (Bistrais and State of Maine, 2025) was clipped to the revised study area. Though the most comprehensive publicly available dataset for the region, this public road network is locally known to omit roads used for private and industry use. To help identify additional road-stream crossings, the team considered areas that have the potential for these additional roads by reclassifying land cover values within the U.S. Geological Survey's (2024) land use/land cover dataset as shown in Table 11. The team applied the *Raster to Polyline* tool to convert the reclassified raster values to gridded polyline areas that approximate where additional roads may exist. To remove any roads already captured within existing data, the team applied a buffer of 100 m to the emergency 911 roads dataset, and then removed any duplicated roads, resulting in a **modeled roads** dataset (polylines).

Using the stream network dataset from the U.S. Geological Survey (2023a), the research team then identified all potential crossings at road and stream intersections within the stream network, emergency 911 roads, and modeled roads datasets. Newly identified road-stream crossing points were then merged with clipped existing point-data crossings from the Maine Stream Habitat Viewer (Gallagher and State of Maine, 2022) and two culvert datasets from the Maine Department of Transportation (Spears and State of Maine, 2021a, 2021b), resulting in a **comprehensive road-stream crossings** dataset (points). This dataset uses a deliberately inclusive approach to identify potential road-stream crossings, prioritizing completeness over precision to minimize omission errors. Because each pre-merged dataset includes spatially explicit points, some clusters may reflect duplicate records of the same crossing, while others may represent multiple nearby culverts. For visualization, the *Kernel Density* tool was used to develop a heat map of road-stream crossings, resulting in a **road-stream crossing density** map in 30×30-m resolution.

Table 11. *Land use/land cover type reclassification crosswalk for road identification.*

Land Use/Land Cover Value	Reclassified Value for Road Identification
11 (Open Water)	NoData
21 (Developed, Open space)	1
22 (Developed, Low Intensity)	1
23 (Developed, Medium Intensity)	1
24 (Developed, High Intensity)	NoData
31 (Barren Land, Rock/Sand/Clay)	1
41 (Deciduous)	NoData
42 (Evergreen Forest)	NoData
43 (Mixed Forest)	NoData
52 (Shrub/Scrub)	NoData
72 (Sedge/Herbaceous)	NoData
81 (Pasture/Hay)	NoData
82 (Cultivated Crops)	NoData
90 (Woody Wetlands)	NoData
95 (Emergent Herbaceous Wetlands)	NoData

Figure 2 displays the final weighting decisions and index development methodology for the final risk index. The stormwater flood hazard index from Section 3.4 and the final soil erodibility index from Section 3.7.1 were equally weighted to create a **stormwater/erodibility index** in 30×30-m resolution. The team then created the final **road-stream crossing risk index** (points), by extracting raster values from the combined stormwater flooding and soil erodibility index at each point location within the comprehensive road-stream crossings dataset. Every road-stream crossing has a resulting risk value from 1–7, where higher values equal higher risk due to stormwater flooding and soil erosion potential. For added benefit, individual crossing risk indices were also developed using the same approach on the stormwater flood hazard and soil erodibility indices to produce a **road-stream crossing risk index** – **stormwater flooding only** (points) and **road-stream crossing risk index** – **soil erodibility only** (points).

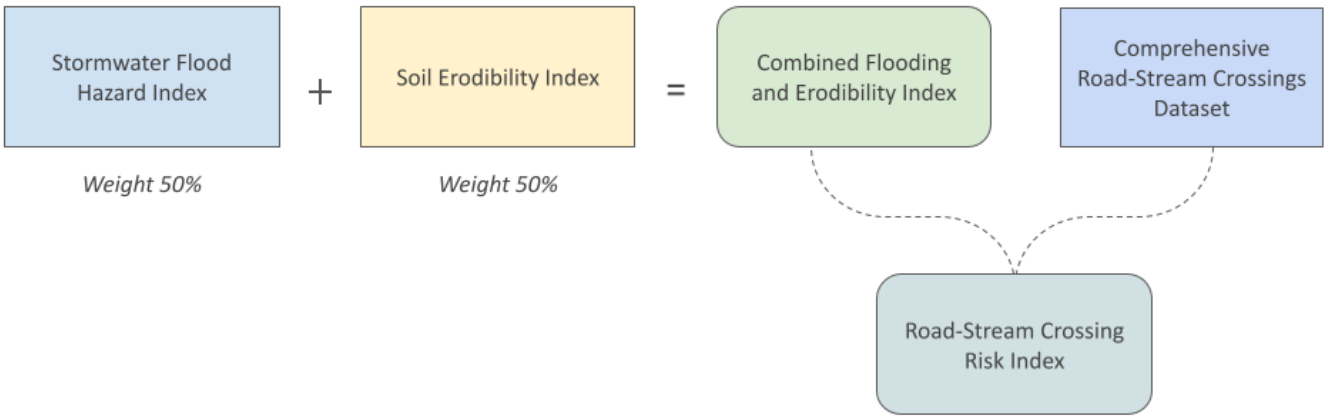

Figure 2. *Conceptual framework for road-steam crossings risk index weighting and integration.*

3.9 Community Isolation Risk

The research team assessed three types of community isolation risks by analyzing street network data, connectivity, hazards, and critical infrastructure to develop indices of road isolation, hazard road isolation risk, and service area isolation risk (Figure 3).

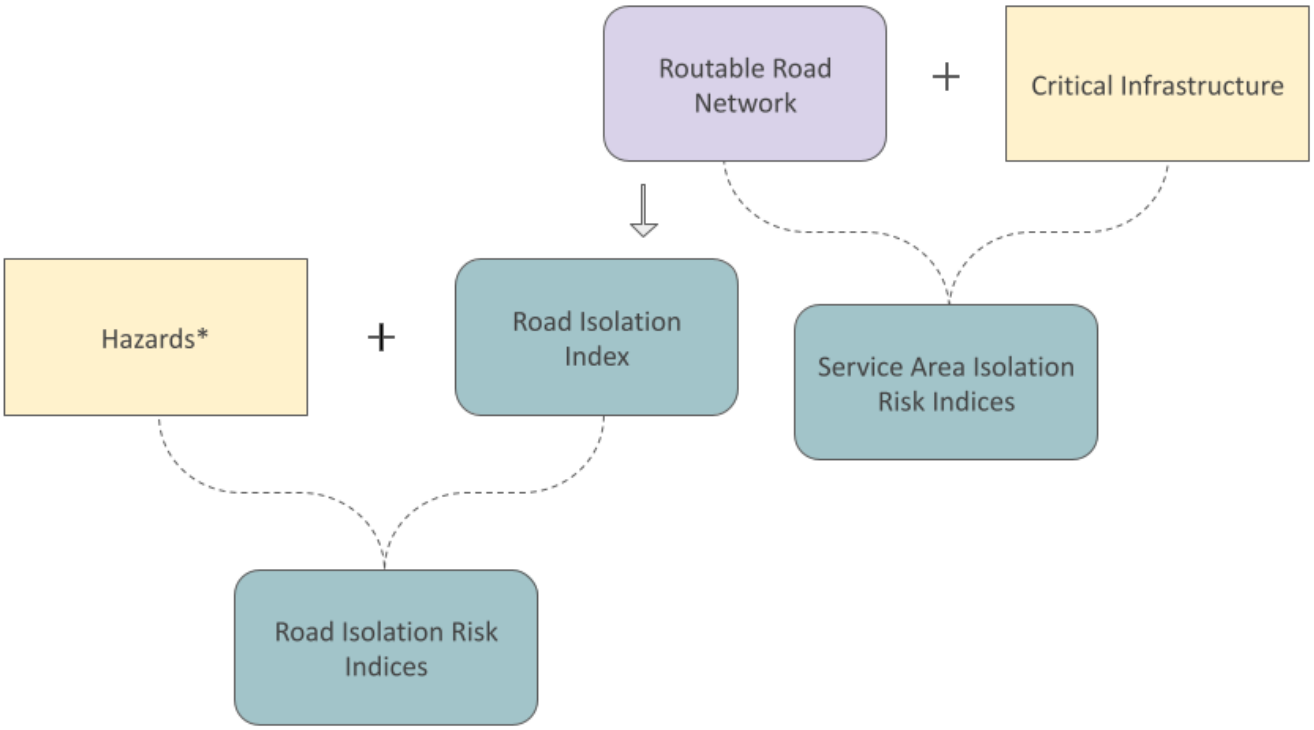

Figure 3. *Community isolation risk analysis conceptual diagram.*

First, the team calculated a **routable road network** (file geodatabase network dataset) by identifying **routable roads** (polyline) and **routable road junctions** (point) through the *Network Analyst* extension, applied to Maine Emergency 911 roads (Bistrais and State of Maine, 2025).[3] This routable road network dataset incorporated accurate connectivity, directionality attributes, speed limits, distance, and network topology, and excluded any disconnected network roads (i.e., islands without connecting roadways or connected by ferry). To avoid forcing routes to stay entirely within the study area—potentially resulting in long or unrealistic detours—a 50-km buffer was added beyond the study area. This allowed the routing algorithm to find the most efficient path, even if it temporarily exited the study area and re-entered at a closer or more logical point. Routes through Canada were excluded to ensure consistent accessibility for all network users, as border crossings are not always reliably available.

Next, network vulnerability was assessed by performing a topological connectivity assessment. The junctions previously created at all nodes within the routable road network were used to calculate the number of proximal connections at each node through spatial joins. Following prior studies that analyzed road network fragility and accessibility impacts at the community scale (Sugiura and Kurauchi, 2023) and to ensure meaningful assessment of local connectivity, the total number of connecting nodes per road segment was calculated. Each road segment was given a connectivity score, calculated by summing the number of other road segments connected at each end (node) of the segment (Redzuan et al., 2022). This score provides a straightforward measure of how well each segment is connected within the local road network. Segments within the resulting **road segment isolation index** (polyline) with low connectivity scores are more susceptible to isolation under hazard conditions, as fewer connections make rerouting more difficult if a segment is closed.

To incorporate hazard exposure (Arango et al., 2023; Mossoux et al., 2019), the stormwater flood hazard index (Section 3.4), winter ice storm hazard index (Section 3.5), wildfire hazard index (Section 3.6), and combined flooding and erodibility index (Section 3.7.3) were then individually intersected with the road segment isolation index.[4] Since road-stream crossings were assigned risk values based on the combined flooding and erodibility index (Section 3.7.3), this index was similarly used in the present analysis to estimate road isolation risk from adverse impacts to road-stream crossings. For each hazard, exposure values were assigned to each road segment using the mean of bilinearly interpolated raster cell values from the hazard layer. Segments intersecting high-severity hazard zones received higher exposure scores, while those intersecting low-severity hazard zones received lower scores. Scores were then rescaled from 0–1 using min-max normalization. For each road segment, its resulting exposure score was then added to its road segment isolation index score, resulting in indices of **stormwater flooding road isolation risk**, **winter ice storm road isolation risk**, **wildfire road isolation risk**, and **road-stream crossings road isolation risk**, all from 0–2 (polyline). A final composite index was created by summing the scores for all four hazard road isolation risk indices, resulting in a **compounded hazard road isolation risk index**, ranging from 0–4 (polyline).[5] While it is unlikely that a single road segment would be

[3] The modeled roads dataset from Section 3.7.2 was not incorporated because its gridded polyline area coverage was not compatible with ESRI's network analysis framework.

[4] Because spatial overlap between the storm surge hazard index and the routable road network were limited, the storm surge hazard index (Section 3.3) was omitted from community isolation risk analyses. Please see Sections 3.7 (Structural Risk by Hazard) and 3.10 (Co-occurrence through Bivariate Choropleth Mapping) for integration of storm surge hazard.

[5] Note that the stormwater flood hazard is included in both the stormwater flooding road isolation risk index and the combined flooding and erodibility road isolation risk index. This places a stronger focus on stormwater flooding impacts, per partner recommendation.

simultaneously impacted by all included hazards, this index provides a holistic overview of which road segments are generally more vulnerable throughout the year. It also accounts for the increased risk of cumulative impacts arising when a road segment affected by one hazard is subsequently exposed to additional hazards prior to the completion of restoration efforts.

Lastly, select critical infrastructure (Table 12) from the structural index (Section 3.2) was mapped to investigate service area isolation. The analysis assessed proximity and access under hazard conditions to identify facilities at risk of isolation—particularly those relying on a few vulnerable road segments (Balasubramani et al., 2016). This is not an emergency response plan, but a general assessment of road network isolation and service area accessibility. The service area analysis was conducted for each critical infrastructure category using the *Service Area* tool within the *Network Analyst* extension. Travel distances (i.e., road network distances rather than straight-line distances) were calculated from each critical infrastructure facility. Distances were measured outward along the road network in 10-km increments, and each road segment was assigned to a distance band (e.g., 0–10 km, 10–20 km) based on its travel distance to the nearest facility within each category. These distance bands were used to identify road segments that are more or less isolated from critical infrastructure, resulting in polyline indices of **health-based service area isolation risk**, **order/safety-based service area isolation risk**, and **services-based service area isolation risk**. Segments located farther from facilities have higher likelihood of isolation under hazard conditions. The three resulting indices were then combined into an **overall service area isolation risk index** (polyline).

Table 12. *Select critical infrastructure by category to inform service area isolation.*

Category	Critical Infrastructure Type
Health	Hospitals
	Assisted living and nursing homes
	Recovery treatment health providers
	Psychiatry providers
	Public health offices
Order and safety	County emergency management agencies
	Fire stations
	EMS stations
	Law enforcement
	Correctional facilities
	Ambulances
Services	Gas stations
	Grocery stores

3.10 Co-occurrence through Bivariate Choropleth Mapping

Finally, the research team developed a series of bivariate choropleth maps to explore additional spatial relationships. Bivariate choropleth mapping is a relationship mapping technique that illustrates two variables simultaneously through different sets of symbols or colors. These maps allow viewers to assess how two

variables change in relation to each other within a study area (ESRI, 2022). For example, a bivariate choropleth map of stormwater flood hazard and storm surge hazard would highlight areas of hazard co-occurrence. Summarized in Table 13, the research team selected the following assessment components: population density (Section 3.1), storm surge hazard (Section 3.3), stormwater flood hazard (Section 3.4), winter ice storm hazard (Section 3.5), wildfire hazard Section 3.6), and soil erodibility (Section 3.7.1). For components that were not already normalized from 0–1, the research team rescaled those indices using min-max normalization. All selected components were then reclassified through grouping by quantile into three classes, resulting in six reclassified indices (30×30-m resolution): **population density index by group class, storm surge hazard index by group class, stormwater flood hazard index by group class, winter ice storm hazard index by group class, wildfire hazard index by group class,** and **soil erodibility index by group class.** For final bivariate creation, the team combined each reclassified index pair and symbolized using the associated raster index values (binned from 1–3) and legend descriptions (Table 14).

Table 13. *Index pairs used for bivariate choropleth creation.*

Component 1	Component 2
Population density	Storm surge hazard
	Stormwater flood hazard
	Winter ice storm hazard
	Wildfire hazard
	Soil erodibility
Storm surge	Stormwater flood hazard
	Soil erodibility

Table 14. *Bivariate choropleth values crosswalk.*

Component 1 Value	Component 2 Value	Legend Description
1	1	Low
1	2	Low/Medium
1	3	Low/High
2	1	Medium/Low
2	2	Medium
2	3	Medium/High
3	1	High/Low
3	2	High/Medium
3	3	High

Workshop mapping exercise. Credit: Reilee Gunsher (CSS/NOAA NCCOS).

4. References

Arango, E., Nogal, M., Sousa, H. S., Matos, J. C., and Stewart, M. G. (2023). GIS-based methodology for prioritization of preparedness interventions on road transport under wildfire events. *International Journal of Disaster Risk Reduction*, *99*, 104126. https://doi.org/10.1016/j.ijdrr.2023.104126

Balasubramani, K., Gomathi, M., and Prasad, S. (2016). GIS-based service area analysis for optimal planning strategies: A case study of fire service stations in Madurai city. *Geographic Analysis*, *5*(2), 11-18.

Bistrais, B., and State of Maine. (2021a). *Maine Correctional Facilities GeoLibrary*. https://maine.maps.arcgis.com/home/item.html?id=6bbbd8c02f0e449db4bd8e17caf48c1d

Bistrais, B., and State of Maine. (2021b). *Maine Libraries GeoLibrary.* https://maine.maps.arcgis.com/home/item.html?id=de89492ad04d49fe8e5761d0c7b7b1da

Bistrais, B., and State of Maine. (2021c). *MaineSociety Cemeteries.* https://www.arcgis.com/home/item.html?id=ea5e07b7956f4efaa466d42c10dd23bf

Bistrais, B., and State of Maine. (2021d). *Point locations of skilled nursing homes in Maine mapped at a scale of 1:24,000.* https://maine.maps.arcgis.com/home/item.html?id=1a0c9c7f3dd04ece88305b4ffd4db73f

Bistrais, B., and State of Maine. (2022). *MaineFacilitiesStructuresNG911.* https://maine.hub.arcgis.com/maps/maine::mainefacilitiesstructuresng911-1/about

Bistrais, B., and State of Maine. (2025). *Maine E911 Roads Feature.* https://maine.hub.arcgis.com/datasets/1436fb9a986c445ea803a90865bd4b51_0/explore?location=45.114287%2C-69.006891%2C7.00

Conkle, C., Moyer, J., Willardson, B., Walden, A., and Nasseri, I. (2006). Hydrology Manual. *L.A. County Department of Public Works Water Resources Division.* https://dpw.lacounty.gov/wrd/publication/engineering/2006_Hydrology_Manual/2006%20Hydrology%20Manual-Divided.pdf

Cortinas Jr., J. V., Bernstein, B. C., Robbins, C. C., and Walter Strapp, J. (2004). An Analysis of Freezing Rain, Freezing Drizzle, and Ice Pellets across the United States and Canada: 1976–90. *Weather and Forecasting*, *19*(2), 377–390. https://doi.org/https://doi.org/10.1175/1520-0434(2004)019<0377:AAOFRF>2.0.CO;2

DeGaetano, A. T., Hirsch, M. E., and Colucci, S. J. (2002). Statistical Prediction of Seasonal East Coast Winter Storm Frequency. *Journal of Climate*, *15*(10), 1101–1117. https://doi.org/10.1175/1520-0442(2002)015<1101:SPOSEC>2.0.CO;2

Degelia, S. K., Christian, J. I., Basara, J. B., Mitchell, T. J., Gardner, D. F., Jackson, S. E., Ragland, J. C., and Mahan, H. R. (2016). An overview of ice storms and their impact in the United States. *International Journal of Climatology*, *36*(8). https://doi.org/10.1002/joc.4525

ESRI. (2022). *Create a quantitative bivariate map in ArcGIS Pro*. Retrieved 16 July 2025 from https://support.esri.com/en-us/knowledge-base/how-to-create-a-quantitative-bivariate-map-in-arcgis-pr-000027489

ESRI. (2023). *Creating Composite Indices Using ArcGIS: Best Practices.* ESRI technical paper, May 2024. https://www.esri.com/content/dam/esrisites/en-us/media/technical-papers/creating-composite-indices-using-arcgis.pdf

ESRI ArcGIS REST Services Directory. (2024). *National_Register_of_Historic_Places_Points.* https://services2.arcgis.com/FiaPA4ga0iQKduv3/ArcGIS/rest/services/nrhp_points_v1/FeatureServer/0

ESRI ArcGIS REST Services Directory. (2025). *Dams.* https://services2.arcgis.com/FiaPA4ga0iQKduv3/arcgis/rest/services/NID_v1/FeatureServer/0

ESRI Business Analyst Data Axle. (2024a). *ESRI Business Analyst, Data Axle, NAICS code 44414005.* https://doc.arcgis.com/en/esri-demographics/latest/arcgis-places/data-axle.htm

ESRI Business Analyst Data Axle. (2024b). *ESRI Business Analyst, Data Axle, NAICS code 44511003.* https://doc.arcgis.com/en/esri-demographics/latest/arcgis-places/data-axle.htm

ESRI Business Analyst Data Axle. (2024c). *ESRI Business Analyst, Data Axle, NAICS code 45712003.* https://doc.arcgis.com/en/esri-demographics/latest/arcgis-places/data-axle.htm

ESRI Business Analyst Data Axle. (2024d). *ESRI Business Analyst, Data Axle, NAICS code 49111001.* https://doc.arcgis.com/en/esri-demographics/latest/arcgis-places/data-axle.htm

ESRI Business Analyst Data Axle. (2024e). *ESRI Business Analyst, Data Axle, NAICS code 81231001.* https://doc.arcgis.com/en/esri-demographics/latest/arcgis-places/data-axle.htm

ESRI Business Analyst Data Axle. (2024f). *ESRI Business Analyst, Data Axle, NAICS codes 62111207, 62221002, 62221003*. https://doc.arcgis.com/en/esri-demographics/latest/arcgis-places/data-axle.htm

ESRI Business Analyst Data Axle. (2024g). *ESRI Business Analyst, Data Axle, NAICS codes 81331106, 81331904, 81331905, 81331906, 81331913.* https://doc.arcgis.com/en/esri-demographics/latest/arcgis-places/data-axle.htm

Fleming, C. S., Dillard, M. K., Regan, S. D., Gorstein, M., Messick, E., and Blair, A. (2017). A coastal community vulnerability assessment for the Choptank Habitat Focus Area. https://doi.org/10.7289/V5/TM-NOS-NCCOS-225

Fleming, C. S., Regan, S. D., Freitag, A., Aslam, U., and Burkart, H. (2024). A Community vulnerability assessment to flood hazard in the U.S. Virgin Islands. NOAA Technical Memorandum NOS NCCOS 344. https://repository.library.noaa.gov/view/noaa/66566

Fleming, C. S., Regan, S. D., Freitag, A., and Burkart, H. (2020). Assessing the Geographic Variability in Vulnerability to Climate Change and Coastal Hazards in Los Angeles County, California. NOAA Technical Memorandum NOS NCCOS 75. https://doi.org/10.25923/mgca-hc06

Gallagher, M., and State of Maine. (2022). *Crossings.* https://maine.hub.arcgis.com/datasets/maine::maine-stream-habitat-viewer/about?layer=0

Hauer, R. J., Dawson, J. O., and Werner, L. P. (2006). Trees and ice storms: The development of ice storm–resistant urban tree populations.

Irland, L. C. (2000). Ice storms and forest impacts. *Science of the total environment*, *262*(3), 231–242.

Isaacs, R. E., Stueve, K. M., Lafon, C. W., and Taylor, A. H. (2014). Ice storms generate spatially heterogeneous damage patterns at the watershed scale in forested landscapes. *Ecosphere*, *5*(11), art141. https://doi.org/10.1890/ES14-00234.1

Jenson, S. K., and Domingue, J. O. (1988). Extracting topographic structure from digital elevation data for geographic information system analysis. *Photogrammetric engineering and remote sensing*, *54*(11), 1593–1600.

Johnson, T., and Sunrise County Economic Council. (2025). *Public Services_WFL1.* https://www.arcgis.com/home/item.html?id=7536300cd3b1431e884fff681f09796f

Kazakis, N., Kougias, I., and Patsialis, T. (2015). Assessment of flood hazard areas at a regional scale using an index-based approach and Analytical Hierarchy Process: Application in Rhodope-Evros region, Greece. *Science of the Total Environment*, *538*, 555–563. https://doi.org/10.1016/j.scitotenv.2015.08.055

Maine Federation of Farmers Markets. (2025). *Markets by Day.* https://mainefarmersmarkets.org/shoppers/markets-by-day/

McCray, C. D., Atallah, E. H., and Gyakum, J. R. (2019). Long-Duration Freezing Rain Events over North America: Regional Climatology and Thermodynamic Evolution. *Weather and Forecasting*, *34*(3), 665–681. https://doi.org/https://doi.org/10.1175/WAF-D-18-0154.1

Mossoux, S., Kervyn, M., and Canters, F. (2019). Assessing the impact of road segment obstruction on accessibility of critical services in case of a hazard. *Natural Hazards and Earth System Sciences*, *19*(6), 1251–1263. https://doi.org/10.5194/nhess-19-1251-2019

National Resources Conservation Service Soil Survey Staff. (2023). *Web Soil Survey.* https://websoilsurvey.nrcs.usda.gov/

National Weather Service. (2024). *January 10 and 13 Coastal Flood Reports, and Observed Water Levels*. National Oceanic and Atmospheric Administration. Retrieved 21 April 2025 from https://www.weather.gov/car/CoastalFloodingSummary

National Weather Service. (n.d.). *Winter Precipitation Types*. Retrieved 21 April 2025 from https://www.weather.gov/ama/preciptypes#:~:text=In%20fact%2C%20there%20is%20a,profile%20supportive%20of%20freezing%20rain

NOAA National Centers for Coastal Ocean Science. (2025). *Community Risk Assessment Portfolio: Glossary*. https://cdn.coastalscience.noaa.gov/projects-attachments/480/Risk-Assessment-Portfolio-Glossary.pdf

NOAA National Hurricane Center. (n.d.). *National Storm Surge Risk Maps - Version 3*. Retrieved 19 September 2025 from https://www.nhc.noaa.gov/nationalsurge/#:~:text=The%20process%20to%20create%20storm,a%20seamless%20raster%20of%20inundation

Panda, S. S., Amatya, D. M., Grace, J. M., Caldwell, P., and Marion, D. A. (2022). Extreme precipitation-based vulnerability assessment of road-crossing drainage structures in forested watersheds using an integrated environmental modeling approach. *Environmental Modelling & Software*, *155*, 105413. https://doi.org/10.1016/j.envsoft.2022.105413

Pettit, E., and State of Maine. (2021a). *Maine State Boundary Polygon Feature.* https://maine.hub.arcgis.com/datasets/0a5e9f2b9c444da3b4e96683f1afecf4/explore?location=45.217364%2C-68.844640%2C7.46

Pettit, E., and State of Maine. (2021b). *Maine Town and Townships Boundary Polygons Feature.* https://maine.hub.arcgis.com/maps/289a91e826fd4f518debdd824d5dd16d/about

Pettit, E., and State of Maine. (2025). *Maine E911 Addresses, Roads, Structure, and PSAP FGDB.* https://maine.maps.arcgis.com/home/item.html?id=f0f136a298534f5e87f8829c003bf12f

PRISM Climate Group at Oregon State University. (2022a). *United States Average Annual Total Precipitation, 1991-2020.* https://www.prism.oregonstate.edu/normals/

PRISM Climate Group at Oregon State University. (2022b). *United States Average December Daily Mean Temperature, 1991-2020.* https://www.prism.oregonstate.edu/normals/

PRISM Climate Group at Oregon State University. (2022c). *United States Average December Total Precipitation, 1991-2020.* https://www.prism.oregonstate.edu/normals/

PRISM Climate Group at Oregon State University. (2022d). *United States Average February Daily Mean Temperature, 1991-2020.* https://www.prism.oregonstate.edu/normals/

PRISM Climate Group at Oregon State University. (2022e). *United States Average February Total Precipitation, 1991-2020.* https://www.prism.oregonstate.edu/normals/

PRISM Climate Group at Oregon State University. (2022f). *United States Average January Daily Mean Temperature, 1991-2020.* https://www.prism.oregonstate.edu/normals/

PRISM Climate Group at Oregon State University. (2022g). *United States Average January Total Precipitation, 1991-2020.* https://www.prism.oregonstate.edu/normals/

Redzuan, A. A. H., Zakaria, R., Anuar, A. N., Aminudin, E., and Yusof, N. M. (2022). Road Network Vulnerability Based on Diversion Routes to Reconnect Disrupted Road Segments. *Sustainability*, *14*(4), 2244. https://www.mdpi.com/2071-1050/14/4/2244

Santom, E. (2025). *How high tides, unusual winds led to historic flooding in January 2024*. Retrieved 11 August 2025 from https://wgme.com/news/local/how-high-tides-and-unusual-winds-led-to-historic-flooding-in-january-2024-winter-storm-damage

Scott, J. H., Dillon, G. K., Jaffe, M. R., Vogler, K. C., Olszewski, J. H., Callahan, M. N., Karau, E. C., Lazarz, M. T., Short, K. C., Riley, K. L., Finney, M. A., and Grenfell, I. C. (2024). *Wildfire Risk to Communities: Spatial datasets of landscape-wide wildfire risk components for the United States (2nd Edition).* https://doi.org/10.2737/RDS-2020-0016-2

Sharma, A., and Tiwari, K. (2019). Sink removal from digital elevation model–a necessary evil for hydrological analysis. *Current science*, *117*(9), 1512–1515. https://www.jstor.org/stable/27138488

Spears, B., and State of Maine. (2021a). *MaineDOT Cross Culverts.* https://maine.hub.arcgis.com/datasets/617d6f95e3e947d7a0d8985ddfc028e9/explore?location=44.711016%2C-67.260680%2C16.85

Spears, B., and State of Maine. (2021b). *MaineDOT Large Culverts.* https://maine.hub.arcgis.com/datasets/05e65c5a43da4f2ab29b88fb33c20a4b_1/explore?location=45.168371%2C-69.011828%2C6.68

State of Maine Geological Survey. (2019). *Maine SLOSH Inundation Depths Category 2.* https://mgs-maine.opendata.arcgis.com/datasets/maine-slosh-inundation-depths-category-2/explore

Stevens, F. R., Gaughan, A. E., Linard, C., and Tatem, A. J. (2015). Disaggregating Census Data for Population Mapping Using Random Forests with Remotely-Sensed and Ancillary Data. *PLOS ONE*, *10*(2), e0107042. https://doi.org/10.1371/journal.pone.0107042

Sugiura, S., and Kurauchi, F. (2023). Isolation vulnerability analysis in road network: Edge connectivity and critical link sets. *Transportation Research Part D: Transport and Environment*, *119*, 103768. https://doi.org/10.1016/j.trd.2023.103768

Sunrise County Economic Council. (n.d.). *Planning Maps*. Retrieved 10 October 2024 from https://sunrisecounty.org/planning-maps/

U.S. Climate Resilience Toolkit. (2021). *Glossary*. Retrieved 15 May 2024 from https://toolkit.climate.gov/content/glossary

U.S. Climate Resilience Toolkit. (n.d.). *Glossary*. Retrieved 18 June 2025 from https://toolkit.climate.gov/glossary

U.S. Department of Agriculture Natural Resources Conservation Service. (2019a). *Soil Survey Data: Drainage Class (Aroostock County, Maine, Southern Part; Northern Hancock and Western Washington County Area, Maine; Penobscot County, Maine; Washington County Area, Maine).* https://websoilsurvey.sc.egov.usda.gov/App/WebSoilSurvey.aspx

U.S. Department of Agriculture Natural Resources Conservation Service. (2019b). *Soil Survey Data: Hydrologic Soil Group (Aroostock County, Maine, Southern Part; Northern Hancock and Western Washington County Area, Maine; Penobscot County, Maine; Washington County Area, Maine).* https://websoilsurvey.sc.egov.usda.gov/App/WebSoilSurvey.aspx

U.S. Department of Agriculture Natural Resources Conservation Service. (2019c). *Soil Survey Data: Wind Erodibility Group (Aroostock County, Maine, Southern Part; Northern Hancock and Western Washington County Area, Maine; Penobscot County, Maine; Washington County Area, Maine.* https://websoilsurvey.sc.egov.usda.gov/App/WebSoilSurvey.aspx

U.S. Environmental Protection Agency. (2024). *FRS_Interests (FeatureServer).* https://services.arcgis.com/cJ9YHowT8TU7DUyn/arcgis/rest/services/FRS_INTERESTS/FeatureServer

U.S. Geological Survey. (2023a). *Maine NHD State Lakes, Ponds, and Streams.* https://apps.nationalmap.gov/downloader/#/

U.S. Geological Survey. (2023b). *USGS 1 arc-second 45w067 20230302.* https://www.sciencebase.gov/catalog/item/6402dea5d34e69298812c31f

U.S. Geological Survey. (2023c). *USGS 1 arc-second 45w068 20230302.* https://www.sciencebase.gov/catalog/item/6402dea3d34e69298812c31c

U.S. Geological Survey. (2023d). *USGS 1 arc-second 45w069 20230302.* https://www.sciencebase.gov/catalog/item/6402de9dd34e69298812c319

U.S. Geological Survey. (2024a). *USGS 1 arc-second 45w068 20240207.* https://www.sciencebase.gov/catalog/item/65c7110dd34ef4b119cb2bc9

U.S. Geological Survey. (2024b). *USGS 1 arc-second 45w069 20241030.* https://www.sciencebase.gov/catalog/item/67298ca0d34e338a476a334f

U.S. Geological Survey Earth Resources Observation and Science Center. (2024). *Annual National Land Cover Database (NLCD) Collection 1 Products: Land Cover.* https://doi.org/10.5066/P94UXNTS

U.S. Geological Survey The National Map. (2021). *The National Map: National Hydrography Dataset.* https://hydro.nationalmap.gov/arcgis/rest/services/nhd/MapServer

University of Maine Machias. (2020). *Utilities.* https://www.arcgis.com/home/item.html?id=654271541eec433da3c69dfcff045f96

University of Maine Machias. (2021). *Community assets for Washington County Maine.* https://www.arcgis.com/home/item.html?id=64e3cb55989549fc8e7f8971a55ce64b&sublayer=5

Weather Prediction Center. (2025). *The Winter Storm Severity Index (WSSI) Product Description Document (PDD)*. National Oceanic and Atmospheric Administration. https://nsdesk.servicenowservices.com/api/g_noa/nwspc/res2/5db27583876f5a544b0fa8a60cbb3576

Weather Prediction Center. (n.d.). *The Winter Storm Severity Index*. National Oceanic and Atmospheric Administration. Retrieved 21 April 2025 from https://www.wpc.ncep.noaa.gov/wwd/wssi/wssi.php

WorldPop. (2022). *WorldPop Population Density 2000-2020 100m.* https://www.arcgis.com/home/item.html?id=c90197b8948948d7b2194e1b03b11d1e

U.S. Department of Commerce

Howard Lutnick, Secretary

National Oceanic and Atmospheric Administration

Laura Grimm, Under Secretary for Oceans and Atmosphere

National Ocean Service

Nicole LeBoeuf, Assistant Administrator for National Ocean Service

The National Centers for Coastal Ocean Science delivers ecosystem science solutions for stewardship of the nation's ocean and coastal resources in direct support of National Ocean Service (NOS) priorities, offices, and customers to sustain thriving coastal communities and economies. For more information, visit: https://www.coastalscience.noaa.gov/